J Biochem 131, 593–603 (2002)

Inhibition of Proteasomes Induces Accumulation, Phosphorylation, and Recruitment of HSP27 and αB-Crystallin to Aggresomes[1]

Hidenori Ito,*[2] Keiko Kamei,* Ikuko Iwamoto,* Yutaka Inaguma,* Rafael García-Mata,† Elizabeth Sztul,† and Kanefusa Kato*

**Department of Biochemistry, Institute for Developmental Research, Aichi Human Service Center, 713-8 Kamiya, Kasugai, Aichi 480-0392; and †Department of Cell Biology, University of Alabama at Birmingham, Birmingham, Alabama 35924, USA*

Received December 6, 2001, accepted February 8, 2002

Molecular chaperones and the ubiquitin-proteasome pathway are known to participate in the quality control of proteins in cells. In this study, we examined the responses of small heat shock proteins to proteasome inhibitors to clarify their roles under conditions where misfolded proteins are abnormally accumulated. HSP27 and αB-crystallin accumulated in both soluble and, more prominently, insoluble fractions after exposure to MG-132, a proteasome inhibitor. Enhanced expression of mRNAs for HSP27 and αB-crystallin was observed, suggesting transcriptional activation. Phosphorylation of HSP27 and αB-crystallin in cells treated with MG-132 was enhanced concomitantly with activation of p38 and p44/42 MAP kinase pathways. Immunofluorescence analysis revealed that exposure to proteasome inhibitors induced the formation of aggresomes in U373 MG cells, to which HSP27 and αB-crystallin were recruited. However, phosphorylation was not required for this accumulation in aggresomes. Thus, HSP27 and αB-crystallin are increased, phosphorylated and localized in aggresomes when proteasome activity is inhibited.

Key words: aggresome, chaperone, crystallin, phosphorylation, proteasome.

Posttranslational quality control of proteins such as folding, refolding, and degradation are required for the maintenance of cellular functions (*1*). If the systems responsible in individual cells are damaged, functions may be lost and this often leads to serious disease. In fact, abnormal accumulation and aggregation of proteins in intracellular and extracellular lesions are associated with cell death in degenerative conditions such as Alzheimer's, Parkinson's and Huntington's diseases (*2*). Molecular chaperones participate in folding of many proteins under both unstressed and stressed conditions (*3*), and several families are known to exist in mammalian cells including the small heat shock protein (sHSP) family. sHSPs, which have a molecular mass of about 15–30 kDa, share several features: possession of a homologous amino acid sequence called the "α-crystallin domain" (*4*); induction by various stimuli including heat, oxidative reagents and heavy metals (*5, 6*); and phosphorylation in response to various stresses and growth factors (*7, 8*). There are several reports describing relationships between sHSPs and human diseases We previously found levels of HSP27 and αB-crystallin, which are typical sHSPs, to be elevated in brains of patients with Alzheimer's disease (*9*). Similarly, ubiquitinated and phosphorylated αB-crystallin accumulates in Alexander's disease as a component of the Rosenthal fibers in glial cells (*10–12*).

Abnormal proteins in the cytosol and nucleus are degraded primarily through the ubiquitin-proteasome pathway. The proteasome is a large multicatalytic complex that catalyzes such degradation (*13*). The pathway is required for the breakdown of many cellular regulatory proteins, and the controlled degradation of substrates is critical for cell survival (*14*). Recently, a variety of reversible (*15*) and irreversible (*16*) proteasome inhibitors have been identified and used to reveal involvement of the ubiquitin-proteasome pathway in diverse cellular functions. Treatment with these proteasome inhibitors activates the heat shock transcription factor (HSF) (*17, 18*) with subsequent induction of heat shock proteins (*19–21*).

In the present study, we examined the responses of sHSPs to proteasome inhibitors to clarify their roles under conditions where misfolded proteins are abnormally accumulated. We found that proteasome inhibitors induce accumulation and phosphorylation of the sHSPs HSP27 and αB-crystallin in U373 MG human glioma cells. Moreover, this was associated with recruitment of HSP27 and αB-crystallin to specialized cellular structures called aggresomes (*22*).

[1]This work was supported in part by Grants-in-Aid for Scientific Research and on Priority Areas (C)-Advanced Brain Science Project from the Ministry of Education, Science, Sports, Culture and Technology of Japan

[2]To whom correspondence should be addressed Tel. +81-568-88-0811 (Ext. 3582), Fax +81-568-88-0829, E-mail: itohide@inst-hsc.pref.aichi.jp

Abbreviations CFTR, cystic fibrosis transmembrane conductance regulator; DMEM, Dulbecco's modified Eagle's medium, EMEM, Eagle's minimal essential medium, GFAP, glial fibrillary acidic protein, HSC, heat shock cognate protein, HSF, heat shock factor; HSP, heat shock protein, IEF, isoelectric focusing; JNK, c-Jun N-terminal kinase, MAP kinase, mitogen-activated protein kinase, MAPKAP kinase, MAP kinase–activated protein kinase, NP-40, Nonidet P-40, PBS, phosphate-buffered saline, PMP22, peripheral myelin protein 22, PRAK, p38 regulated/activated protein kinase, sHSP, small heat shock protein

MATERIALS AND METHODS

Reagents—MG-132 was purchased from Calbiochem-Novabiochem (La Jolla, CA) or Peptide Institute. (Osaka). Lactacystin, SB203580, PD169316, and PD98059 were obtained from Calbiochem-Novabiochem. Carbobenzoxy-L-leucyl-L-leucinal was obtained from Peptide Institute. Uo126 was purchased from Promega (Madison, WI). Mouse monoclonal antibodies against vimentin (Sigma Chemical, St Louis, MO), against ubiquitin (Medical and Biological Laboratories, Nagoya), against 20S proteasome (*23*) (generously provided by Dr. K. Tanaka, Tokyo Metropolitan Institute of Medical Science, Tokyo) and against β-tubulin (Boehringer Mannheim, Germany) were used. Rabbit polyclonal antibodies against p38 mitogen-activated protein (MAP) kinase, phospho-p38 MAP kinase, p44/42 MAP kinase, and phospho-p44/42 MAP kinase were purchased from New England Biolabs. (Beverly, MA). Ampholine for isoelectric focusing (IEF) was obtained from Amersham Pharmacia Biotech (Uppsala, Sweden) and Alexa Fluor 488 goat anti-rabbit and Alexa Fluor 568 goat anti-mouse IgG conjugates from Molecular Probes (Eugene, OR). Okadaic acid and calyculin A were purchased from Wako Pure Chemicals (Osaka).

Cell Culture and Preparation of Cell Extracts—U373 MG human glioma cells were grown in Eagle's minimal essential medium (EMEM; Nissui Pharmaceutical, Tokyo) supplemented with 10% fetal calf serum (Equitech-Bio, Inc., Ingram, TX) at 37°C in a humidified atmosphere of 95% air and 5% CO_2. Cells were seeded on 90-mm dishes. HeLa cells and NG108-15 cells were grown in Dulbecco's modified Eagle's medium (DMEM; Nissui Pharmaceutical). When cells reached confluence, they were treated with various chemicals at 37°C. Cells in each dish were rinsed with phosphate-buffered saline (PBS, containing 8 g of NaCl, 0.2 g of KCl, 1.15 g of $Na_2HPO_4 \cdot 12H_2O$, and 0.2 g of KH_2PO_4 in 1,000 ml of H_2O) and frozen at –80°C for a few days. Cells were collected and suspended in 0.25 ml of a suspension buffer, 50 mM Tris-HCl buffer, pH 7.5, containing 0.1 M NaF, 5 mM EDTA, 0.3 mg/ml Pefablock SC (Roche Diagnostics, IN), 0.2 μM okadaic acid, and 0.2 μM calyculin A (buffer S). Each suspension was sonicated at 0°C for 1 min and centrifuged at 125,000 ×*g* for 20 min at 4°C. The supernatants were used as soluble fractions of cells and the pellets were washed once by sonication and centrifugation with buffer S and then solubilized with 0.1 ml of buffer S containing 2% sodium dodecyl sulfate (SDS) for SDS–polyacrylamide gel electrophoresis (PAGE) or buffer S containing 8 M urea and 0.5% Nonidet P-40 (NP-40) for IEF. For detection of p38 and p44/42 MAP kinases, cells were suspended in buffer S containing 2% SDS and extracts were prepared by sonication and centrifugation as described above.

Preparation and Purification of Antibodies against Phosphorylated HSP27—Two peptides corresponding to internal sequences of human HSP27, containing phosphorylated Ser-15 (residues 10–20, LLRGPSWDPFR; p15S) and Ser-82 (residues 79–89, RQLSSGVSEIR; p82S), respectively, were synthesized. Each peptide was conjugated with hemocyanin (Sigma) using *N*-(4-carboxycyclohexylmethyl)maleimide (Zeiben Chemicals, Tokyo) (*24*) Antisera were raised in rabbits by injection of each conjugate (0.5 mg of peptide/animal), and antibodies were purified with each peptide-coupled Sepharose by the procedures described previously (*25*).

Electrophoresis and Western Blot Analysis—SDS-PAGE was performed as described by Laemmli (*26*) in 12.5% gels. IEF was carried out as described by O'Farrell (*27*) using the Protean II system from Bio-Rad (Hercules, CA) (*28*). We used gels for IEF composed of 9.2 M urea, 2% Ampholine mixture (4 parts Ampholine pH 5–7 and 1 part Ampholine pH 3.5–10 for detection of HSP27, and 4 parts Ampholine pH 6–8 and 1 part Ampholine pH 3.5–10 for detection of αB-crystallin), 4% acrylamide, and 2% NP-40. The proteins in gels were transferred electrophoretically to nitrocellulose sheets (SDS-PAGE) or polyvinylidene difluoride membranes (type GV; Nihon Millipore, Yonezawa) (IEF), incubated at room temperature for 2 h with the primary antibodies, and then for 1 h with the second antibodies. Affinity-purified antibodies raised in rabbits against human HSP27 (*29*), phosphopeptides corresponding to the two phosphorylation sites of human HSP27, the carboxyl-terminal decapeptide of αB-crystallin (*25*) or phosphopeptides corresponding to the three phosphorylation sites of αB-crystallin (p19S, p45S, and p59S) (*28*), were employed as primary antibodies, and peroxidase-labeled antibodies raised in goat against rabbit IgG as the second antibodies. Peroxidase activity on membranes was visualized on X-ray films using a Western blot chemiluminescence reagent (Renaissance, Dupont NEN, Boston, MA). In some experiments, peroxidase activity was also detected with the aid of a luminoimage analyzer LAS-1000 (Fuji Film, Tokyo) and the relative densities of protein bands were quantified with relevant software.

Isolation of RNA and Northern Blot Analysis—Total RNA was isolated from cells with a QuickPrep total RNA Extraction kit (Amersham Pharmacia Biotech), and 10 μg aliquots were subjected to electrophoresis on 0.9% agarose–2.2 M formaldehyde gels and blotted onto nitrocellulose membranes. For Northern blot analysis, membranes were allowed to hybridize with cDNA probes that had been labeled with ^{32}P using a Multiprime DNA labeling system (Amersham Pharmacia Biotech), as described previously (*30*) A *Bam*HI–*Hin*dIII fragment of cDNA for mouse HSP27 (*31*) was kindly provided by Dr. L.F. Cooper, University of North Carolina, and a *Pst*I fragment of cDNA for bovine αB-crystallin (*32*) by Dr H. Bloemendal, University of Nijmegen, The Netherlands. Hybridized membranes were autoradiographed with X-ray film.

Immunofluorescence—U373 MG cells were seeded on glass coverslips and when they reached confluence, they were treated with various chemicals at 37°C. Cells on each coverslip were rinsed twice with PBS, permeabilized with PBS containing 0.5% NP-40 and 5 mM $MgCl_2$ for 1 min at room temperature, washed three times with PBS and fixed with 4% paraformaldehyde in PBS for 30 min at room temperature In control experiments, cells treated with various chemicals were washed with PBS, fixed with 4% paraformaldehyde and permeabilized with 0.2% Triton X-100 in PBS for 15 min at room temperature. Fixed cells were washed three times with PBS and blocked with 10% normal goat serum in PBS containing 0.1% sodium azide for 30 min. Incubation was with primary and secondary antibodies, diluted in 10% normal goat serum in PBS, at room temperature for 2 and 1 h, respectively. In the experiment on the

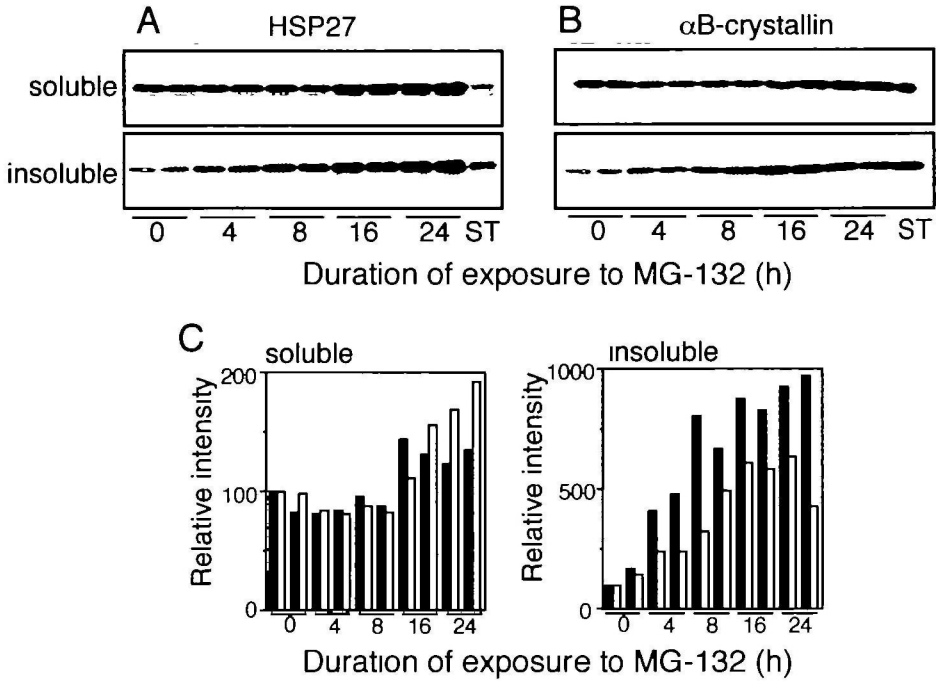

Fig 1 **Accumulation of HSP27 and αB-crystallin in U373 MG cells during exposure to MG-132.** (A) and (B), Five micromolar MG-132 was added to medium of confluent cultures of U373 MG cells followed by incubation at 37°C for the indicated periods Cells were harvested and soluble and insoluble fractions were prepared as described in "EXPERIMENTAL PROCEDURES" Each extract containing 5 μg of proteins was subjected to SDS-PAGE and subsequent Western blot analysis using antibodies against HSP27 (A) and αB-crystallin (B) Two different samples collected at the indicated times were loaded "ST" is a purified standard protein of HSP27 (A) and αB-crystallin (B) (C) Relative densities of protein bands in (A) and (B) were quantified by luminoimage analyzer LAS-1000 The data are shown as percentages relative to the intensity of each at time zero (on the left) Closed bars, HSP27, open bars, αB-crystallin

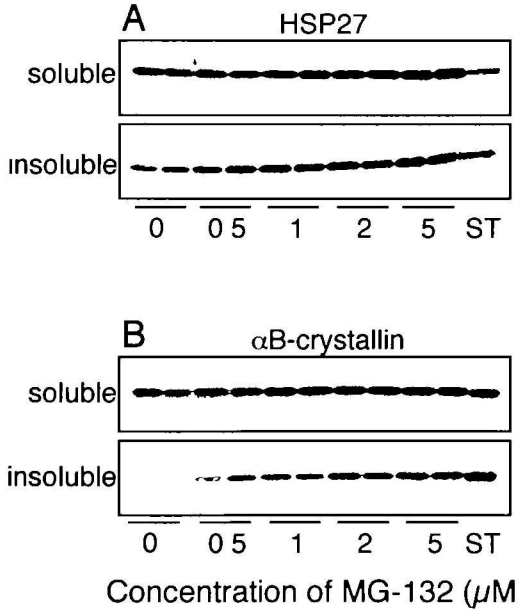

Fig 2 **Dose dependence of MG-132–mediated accumulation of HSP27 and αB-crystallin in U373 MG cells.** Cells were incubated in the presence or absence of the indicated concentrations of MG-132 at 37°C for 16 h Soluble and insoluble fractions of cells were prepared, and extracts containing 5 μg of proteins were subjected to SDS-PAGE and subsequent Western blot analysis using antibodies against HSP27 (A) and αB-crystallin (B) Two different samples treated with the indicated concentrations of MG-132 were loaded "ST" is a purified standard protein of HSP27 (A) and αB-crystallin (B)

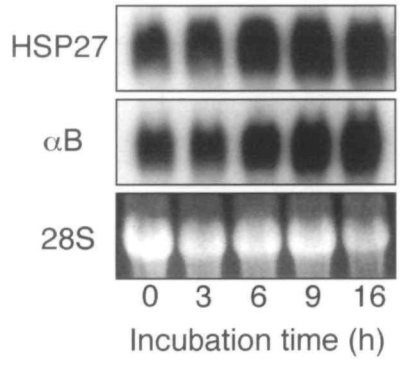

Fig 3 **Northern blot analysis of mRNA for HSP27 and αB-crystallin in U373MG cells treated with MG-132.** Confluent cultures of U373 MG cells were incubated with 5 μM MG-132 at 37°C for the indicated periods. Total RNA was extracted from cells and 10-μg aliquots were subjected to Northern blot analysis of mRNAs for HSP27 and αB-crystallin A photograph of 28S ribosomal RNA is also shown for reference

expression of GFP-250, cells were seeded on coverslips and transiently co-transfected with two plasmids, 1 μg of αB-pCMV5 (*33*) and 1 μg of GFP-250 (*34*), by using LipofectAMINE Plus reagent (Life Technologies, Gaithersburg, MD). Cells were permeabilized and fixed after 24 h and stained as described above. Fluorescent images were obtained using a confocal microscope (FLUOVIEW; Olympus optical, Tokyo).

Other Methods—Human HSP27 was purified from pectoral muscles obtained at surgical resection of breast cancer (*29*). Bovine αB_1-crystallin (phosphorylated form) and αB_2-crystallin (unphosphorylated form) were purified from lens as described previously (*25*). Concentrations of protein were estimated with a micro BCA protein assay reagent kit (Pierce, IL) or a Bio-Rad protein assay kit (Bio-Rad) with bovine serum albumin as the standard.

RESULTS

Proteasome Inhibition Induces Accumulation of HSP27 and αB-Crystallin—The effects of a proteasome inhibitor, MG-132, on the levels of HSP27 and αB-crystallin were examined in U373 MG cells. Since HSP27 and αB-crystallin are known to translocate from the soluble cytosol fraction to the insoluble nuclear/membrane fraction (*35, 36*), we estimated the levels of these proteins in both soluble and insoluble fractions. As shown in Fig 1, A and B, HSP27 and αB-crystallin were present mainly in the soluble fraction in control U373 MG cells. Levels of these proteins increased after addition of MG-132 in both soluble and insoluble fractions, reaching a plateau at 16–24 h (Fig. 1, A and B). The increase in the insoluble fraction was the more prominent (Fig. 1, A and B). Because the ratios of total amounts of proteins in each fraction remained unchanged after expo-

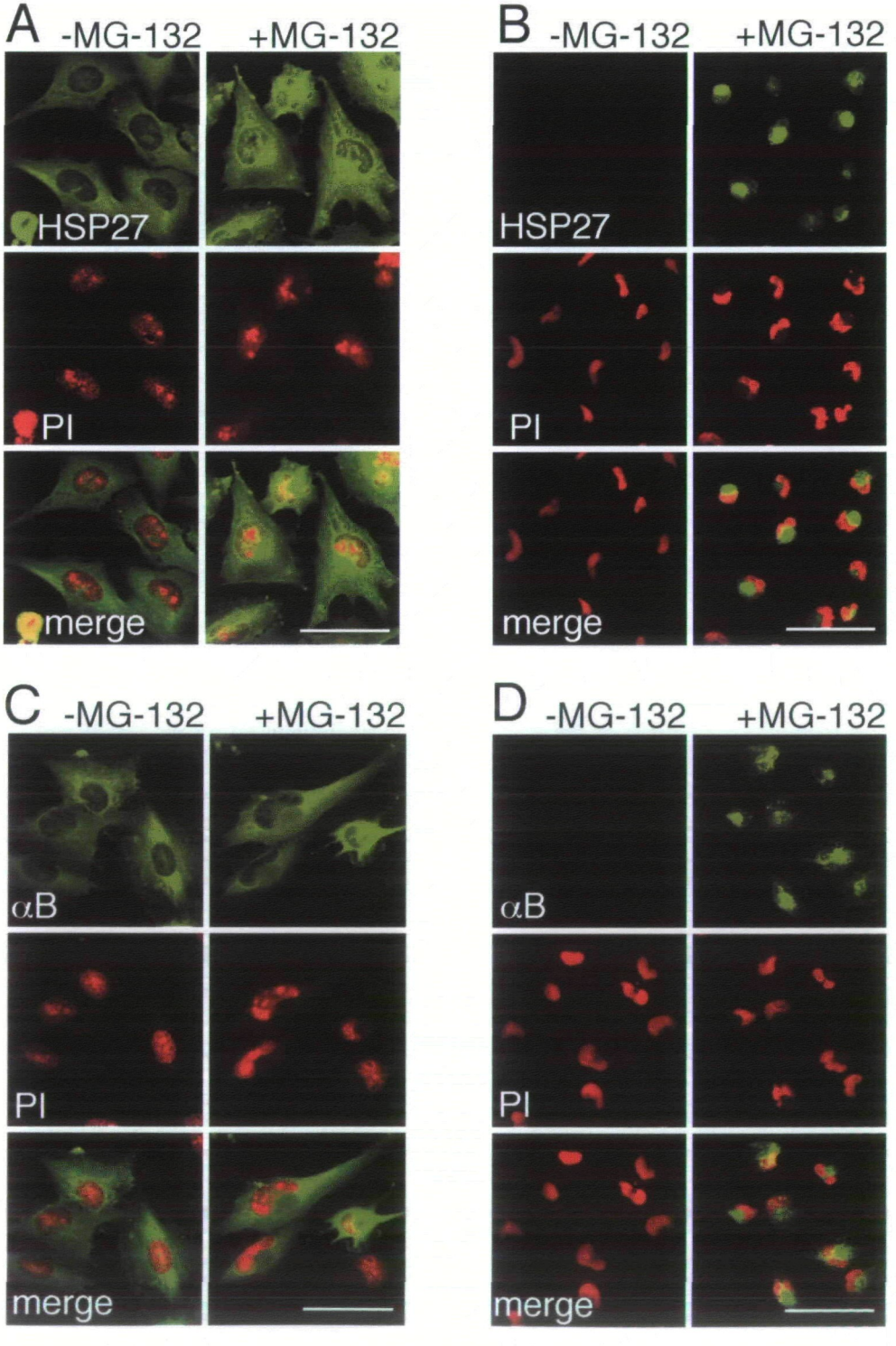

Fig. 4 **Immunocytochemical analysis of HSP27 and αB-crystallin in U373 MG cells exposed to MG-132.** Cells were incubated with or without 5 μM MG-132 at 37°C for 16 h, fixed and then permeabilized (A and C) or permeabilized and then fixed (B and D), and subsequently stained with antibodies against HSP27 (A and B) or αB-crystallin (αB) (C and D) The nuclei were stained with propidium iodide (PI) All images were obtained using confocal microscopy All bars show 50 μm

sure to MG-132 (data not shown), these results indicate that the distributions of HSP27 and αB-crystallin also changed in addition to protein accumulation. The increase in HSP27 and αB-crystallin in U373 MG cells after exposure to MG-132 was confirmed by quantitation of intensities of bands in Fig. 1, A and B, by luminoimage analysis (Fig. 1C). The sHSPs accumulated in U373 MG cells even at a 0.5 μM concentration of MG-132, dose-dependently increased up to 5 μM and reached a plateau (Fig 2). Treatment with higher concentrations (5–20 μM) of MG-132 did not lead to the further increase of HSP27 and αB-crystallin (data not shown). Since MG-132 is also known to inhibit another protease, calpain, we further examined the effects of lactacystin, a more specific proteasome inhibitor (*16*), and carbobenzoxy-L-leucyl-L-leucinal, an inhibitor of calpain but not of proteasomes (*37*), for their ability to increase levels of small heat shock proteins in U373 MG cells. Exposure to 10 μM lactacystin but not 50 μM carboben-

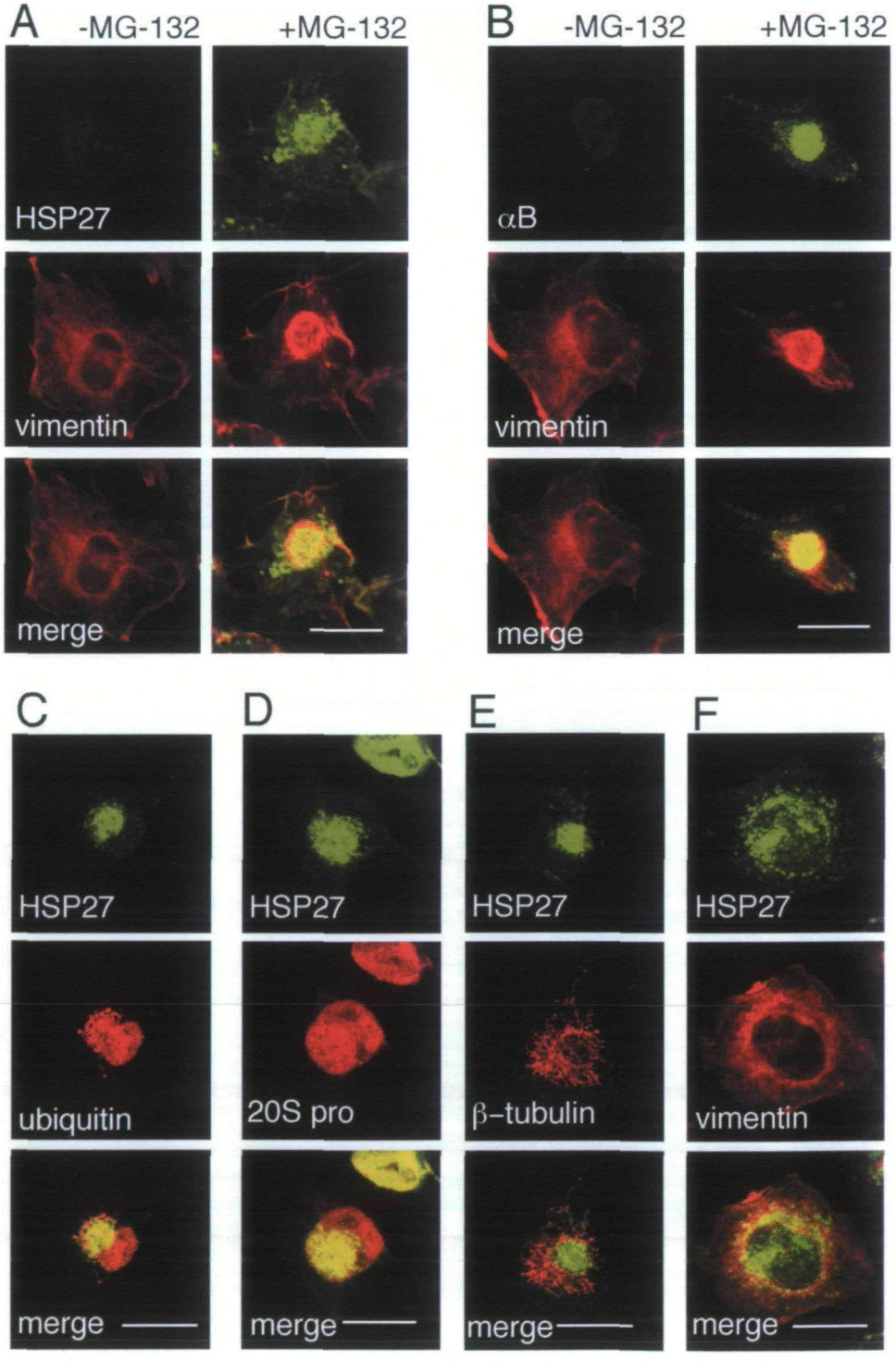

Fig. 5. **Formation of intracellular "aggresomes" is induced in U373 MG cells after exposure to MG-132.** Cells were incubated with or without 5 μM MG-132 at 37°C for 16 h, permeabilized, fixed and stained with antibodies against HSP27 and vimentin (A) or αB-crystallin and vimentin (B). Cells exposed to 5 μM MG-132 were stained with antibodies against HSP27 and ubiquitin (C), HSP27 and 20S proteasomes (20S pro) (D) or HSP27 and β-tubulin (E). Cells incubated with 5 μM MG-132 in the presence of 25 ng/ml nocodazole were stained with antibodies against HSP27 and vimentin (F). All images were obtained using confocal microscopy All bars show 20 μm

zoxy-L-leucyl-L-leucinal caused accumulation of HSP27 and αB-crystallin (data not shown). To examine whether the accumulation induced by exposure to MG-132 was due to transcriptional activation, we estimated levels of mRNAs for HSP27 and αB-crystallin in U373 MG cells by Northern blot analysis. Increase was observed at 6–9 h after exposure to MG-132 and this persisted for up to 16 h (Fig. 3).

HSP27 and αB-crystallin Accumulate in Aggresomes After Exposure to Proteasome Inhibitors—In view of the observed change of the distribution of HSP27 and αB-crystallin, we next determined the cellular localization of HSP27 and αB-crystallin after exposure to MG-132 by immunofluorescence. When we fixed cells prior to permeabilization, HSP27 and αB-crystallin were observed mainly in the cytosol in control U373 MG cells (Fig. 4, A and C, left panel). After treatment with MG-132, both proteins were also seen mainly in the cytosol and to a lesser extent in the nucleus (Fig. 4, A and C, right panel). In contrast, when we permeabilized cells before fixation, staining of HSP27 and αB-crystallin in the cytosol of control cells almost completely disappeared (Fig. 4, B and D, left panel), and intense juxtanuclear staining was observed in 70–90% of cells exposed to MG-132 for 16 h (Fig. 4, B and D, right panel). Similar structures were also observed when cells were treated with lactacystin but not with carbobenzoxy-L-leucyl-L-leucinal (data not shown). Recently, Johnston *et al.* reported expression of misfolded proteins and proteasome inhibition to induce the formation of intracellular inclusions called "aggresomes" (*22*), defined as pericentriolar membrane-free, cytoplasmic inclusions containing misfolded, ubiquitinated proteins ensheathed in a cage of intermediate filaments. Vimentin filaments were observed as reticular elements in control U373 MG cells (Fig. 5, A and B, left panel) Exposure to MG-132 disrupted these reticular structures and caused accumulation of vimentin in a perinuclear region, co-localizing with HSP27 and αB-crystallin (Fig. 5, A and B, right panel). HSP27 also co-localized with ubiquitin (Fig 5C) and 20S proteasomes (Fig. 5D). To define the location of the microtubule-organizing center, we used staining with anti–γ-tubulin antibodies However, we could not clearly detect a positive staining in aggresomes induced in U373 MG cells (data not shown). Therefore, we used staining with anti–β-tubulin antibodies, because microtubules are assembled and radiate from the microtubule-organizing center (*38*). Instead of normal astral distribution, a central hole containing HSP27 is visible in most cells exposed to MG-132, and microtubules extend from the region accumulating HSP27 (Fig. 5E). These results are similar to observations in the previous report (*34*) and suggest that the site accumulating HSP27 is a microtubule-organizing center An intact microtubule-based cytoskeleton is required for the formation of aggresomes (*34*) The microtubule network can be inhibited by microtubule-disrupting reagents (*22*). In our experiment, one such reagent, nocodazole, also blocked the accumulation of small heat shock proteins and vimentin in the juxtanuclear region of cells (Fig. 5F). We also performed the same experiments as described above to characterize the localization of αB-crystallin and we obtained similar results as with the HSP27 case (data not shown). Formation of aggresomes and accumulation of HSP27 in response to proteasome inhibitors were also observed in HeLa cells (Fig. 6A) Moreover, accumulation of αB-crystallin (Fig. 6B) and HSP27 (data not shown) in aggresomes was observed when the formation of

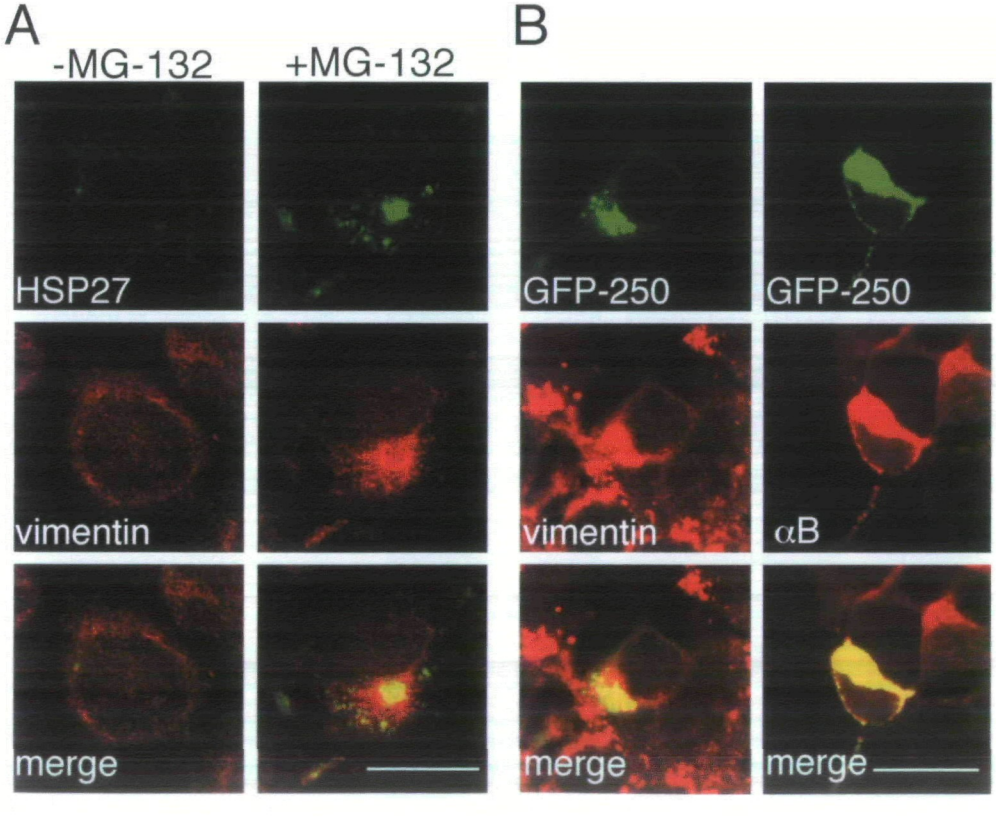

Fig 6 **Formation of aggresomes and accumulation of HSP27 in response to MG-132 in HeLa cells (A) and formation of aggresomes by a misfolded protein, GFP-250, and accumulation of αB-crystallin in NG108-15 cells (B).** (A) HeLa cells were incubated with or without 5 μM MG-132 at 37°C for 16 h, permeabilized, fixed and stained with antibodies against HSP27 and vimentin (B) αB-crystallin and GFP-250 were co-expressed in NG-108-15 cells by transient transfection After 24 h, cells were permeabilized, fixed and stained with antibodies against vimentin or αB-crystallin. All images were obtained using confocal microscopy All bars show 20 μm

aggresomes was induced by expression of misfolded proteins, GFP-250 (*34*), in NG108-15 cells not treated with proteasome inhibitors.

Exposure to Proteasome Inhibitors Induces Phosphorylation of HSP27 and αB-Crystallin—Phosphorylation is one of the most important and characteristic features of small heat shock proteins. In fact, HSP27 and αB-crystallin are phosphorylated in response to various stressful stimuli (*7, 8, 28*). Exposure to MG-132 induced the increase of acidic forms of HSP27. Four isoforms (indicated as p0, p1, p2 and p3; the band "p3" was rather faint and often undetectable) were finally detected after 16–24 h, and the increase was more prominent in the insoluble fraction than in the soluble (Fig. 7A). This result was consistent with a previous description of three phosphorylation sites in the molecule of human HSP27 (*39*). Phosphorylated αB-crystallin was observed in the soluble and to a lesser extent in the insoluble fraction in control cells, and increased in both after treatment with MG-132 (Fig 7B) Phosphorylation of HSP27 and αB-crystallin was also observed when the cells were exposed to lactacystin but not to carbobenzoxy-L-leucyl-L-leucinal (data not shown), indicating that inhibition of proteasome activity was responsible for the enhanced phosphorylation. Using previously produced affinity-purified antibodies that specifically recognize three phosphorylation sites of αB-crystallin (*28*), we determined those with changes in response to proteasome inhibition. As shown in Fig. 7C, αB-crystallin phosphorylated at Ser-45 and Ser-59 was observed in both soluble and insoluble fractions after exposure to MG-132. Phosphorylation of Ser-59 was more prominent. We previously reported that phosphorylation of Ser-45 and Ser-59 in αB-crystallin is catalyzed respectively by p44/42 MAP kinase and MAP kinase–activated protein (MAPKAP) kinase-2, a kinase activated by p38 MAP kinase (*40*). Other groups reported that phosphorylation of HSP27 is catalyzed by MAPKAP kinase-2/3 (*39, 41*) and p38 regulated/activated protein kinase (PRAK) (*42*). Indeed, p44/42 MAP kinase was activated maximally at 4–8 h after exposure to MG-132 (Fig. 8, right panel) and p38 MAP kinase was activated maximally after 16–24 h (Fig. 8, left panel).

Effect of Protein Kinase Inhibitors on the Accumulation, Phosphorylation and Recruitment of HSP27 and αB-Crystallin to Aggresomes—We next estimated the effect of various protein kinase inhibitors on the accumulation and phosphorylation of HSP27 and αB-crystallin Since we have recently produced affinity-purified antibodies that specifically recognize phosphorylated Ser-15 and Ser-82, respectively in Western blot analysis (data not shown; to be described in detail elsewhere), we used these antibodies in this experiment in addition to the phospho-specific antibodies against αB-crystallin. Phosphorylation of Ser-15 and

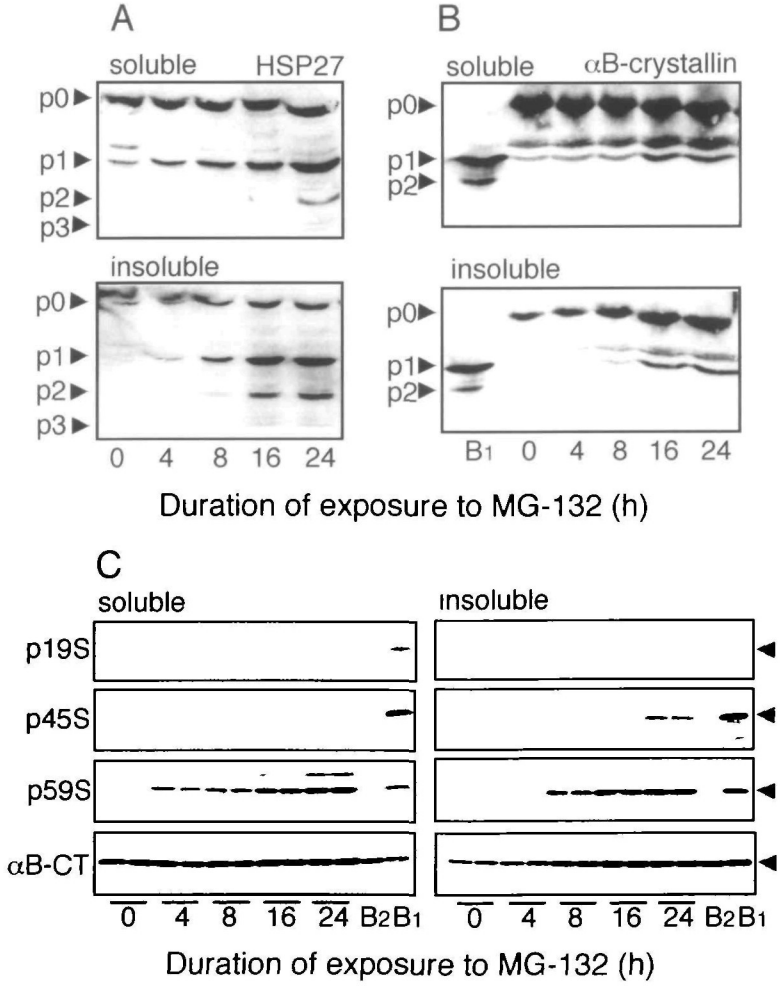

Fig 7 **Phosphorylation of HSP27 and αB-crystallin induced by MG-132.** (A) and (B), Confluent cultures of U373 MG cells were incubated with 5 μM MG-132 at 37°C for the indicated periods. Soluble and insoluble fractions were prepared as described in "EXPERIMENTAL PROCEDURES." Each extract containing 20 μg of protein was subjected to isoelectric focusing and subsequent Western blot analysis using antibodies against HSP27 (A) and αB-crystallin (B) (C) Cells were incubated with 5 μM MG-132 at 37°C for the indicated periods Soluble and insoluble fractions were prepared, and extracts containing 20 μg of protein for detection of phosphorylated αB-crystallin and 5 μg of protein for detection of total αB-crystallin were subjected to SDS-PAGE and subsequent Western blot analysis using antibodies against phosphorylated Ser-19 (p19S), Ser-45 (p45S), Ser-59 (p59S) in αB-crystallin, and the carboxyl terminal of αB-crystallin (αB-CT). Two different samples collected at the indicated times were loaded B_1, phosphorylated form of αB-crystallin purified from bovine lens, B_2, unphosphorylated form of αB-crystallin purified from bovine lens

Ser-82 in HSP27 and Ser-45 and Ser-59 in αB-crystallin was observed in both soluble and insoluble fractions after exposure to MG-132 (Fig. 9). SB203580 and PD169316, which specifically inhibit p38 MAP kinase, significantly, but not completely, inhibited phosphorylation of Ser-15 and Ser-82 in HSP27 and Ser-59 but not Ser-45 in αB-crystallin (Fig. 9). In contrast, Uo126 and PD98059, which specifically inhibit the MEK and suppress activation of p44/42 MAP kinase, significantly inhibited Ser-45 in αB-crystallin (Fig. 9B and data not shown). These results indicate that proteasome inhibitor induces activation of p38 MAP kinase and p44/42 MAP kinase, and activation of these kinases results in the phosphorylation of HSP27 and αB-crystallin.

Although these protein kinase inhibitors differently inhibit the proteasome inhibitor–induced phosphorylation of HSP27 and αB-crystallin, accumulation and change of the distribution of both proteins was barely affected (Fig. 9). Moreover localization of HSP27 (Fig. 10) and αB-crystallin (data not shown) in aggresomes after exposure to MG-132 was barely affected by SB203580 (Fig 10) and PD98059

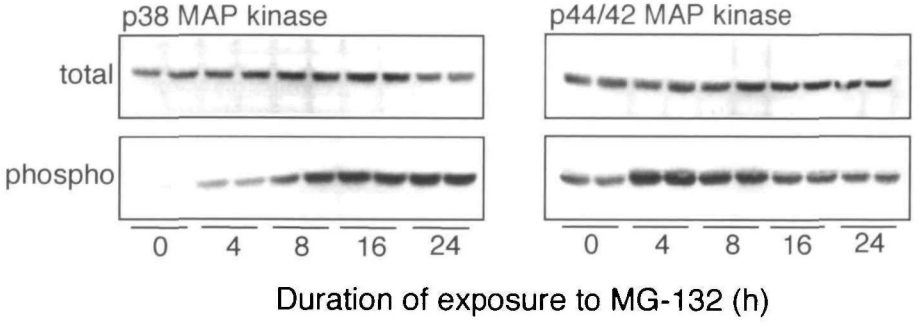

Fig 8. **Exposure to MG-132 caused activation of p38 and p44/42 MAP kinases in U373 MG cells.** U373 MG cells were incubated with 5 μM MG-132 at 37°C for the indicated periods. Total extracts of cells containing 40 μg of protein were subjected to SDS-PAGE and subsequent Western blot analysis using antibodies against p38 or p44/42 MAP kinases (total) and their phosphorylated forms (phospho) Two different samples collected at the indicated times were loaded

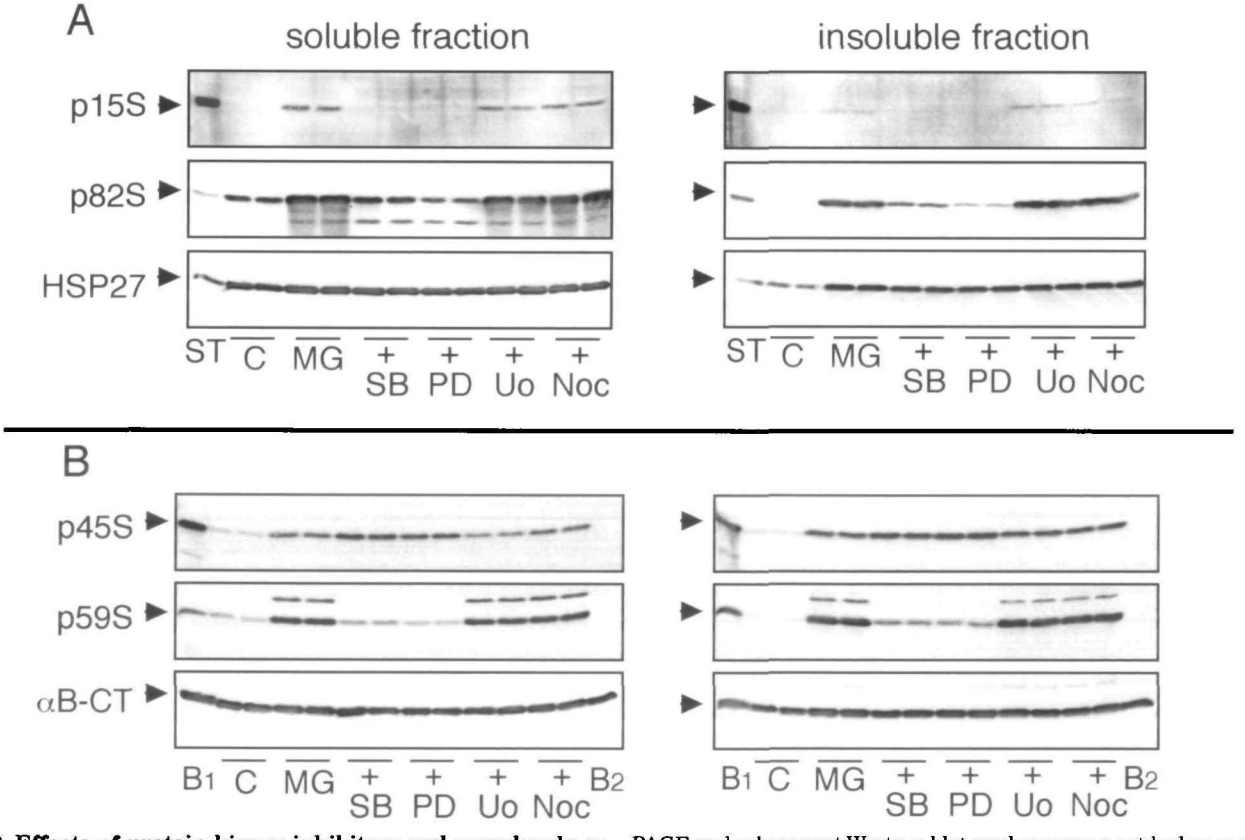

Fig 9. **Effects of protein kinase inhibitors and nocodazole on accumulation and phosphorylation of HSP27 (A) and αB-crystallin (B) in U373 MG cells exposed to MG-132.** Cells were incubated with or without 5 μM MG-132 (MG) in the presence or absence of 10 μM SB203580 (SB), 10 μM PD169316 (PD), 10 μM Uo126, and 25 ng/ml nocodazole (Noc) at 37°C for 16 h. Soluble and insoluble fractions were obtained Extracts containing 20 μg of protein for detection of phosphorylated HSP 27 and αB-crystallin, and 5 μg of protein for detection of total HSP27 and αB-crystallin were subjected to SDS-PAGE and subsequent Western blot analysis using antibodies against phosphorylated Ser-15 (p15S), Ser-82 (p82S) in HSP27 and human HSP27 (A), and phosphorylated, Ser-45 (p45S), Ser-59 (p59S) in αB-crystallin, and the carboxyl terminal of αB-crystallin (αB-CT) (B) Two different samples collected at the indicated times were loaded "ST" stands for purified standard HSP27. B_1, phosphorylated form of αB-crystallin purified from bovine lens; B_2, unphosphorylated form of αB-crystallin purified from bovine lens

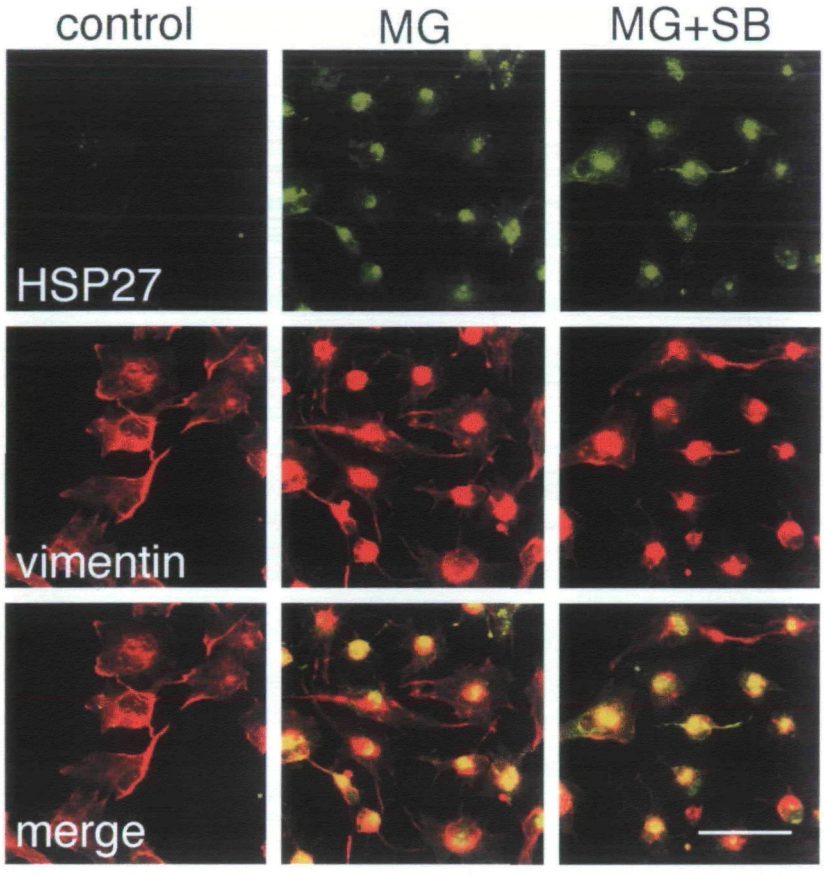

Fig 10 **Effects of SB203580 on formation of aggresomes and localization of HSP27.** Cells were incubated with or without 5 μM MG-132 (MG) in the presence or absence of 10 μM SB203580 (MG+SB) at 37°C for 16 h. Then they were permeabilized, fixed and stained with antibodies against HSP27 and vimentin All images were obtained using confocal microscopy Bar shows 50 μm.

(data not shown). Nocodazole inhibited the formation of aggresomes (Fig. 5) We also determined the effect of nocodazole on the proteasome inhibitor-induced responses of HSP27 and αB-crystallin. As shown in Fig. 9, nocodazole barely affected the accumulation, phosphorylation and change of the distribution of HSP27 and αB-crystallin.

These results indicate that the accumulation, change of the distribution and recruitment to aggresomes of HSP27 and αB-crystallin do not directly correlate with their phosphorylation states.

DISCUSSION

In this study, we found the small heat shock proteins HSP27 and αB-crystallin to be induced, phosphorylated and localized in aggresomes after proteasome inhibition in U373 MG cells. There have been a number of reports describing induction of HSPs by proteasome inhibitors via activation of heat shock transcription factor (HSF) in several mammalian cell lines (*17–21*). In our experiments, HSP27 and αB-crystallin mRNAs were increased (Fig 3). The fact that induction of HSP70 was also observed (data not shown) indicates that activation of HSF might have been involved.

HSP27 and αB-crystallin accumulated in both soluble and, more prominently, in insoluble fractions after exposure to MG-132 (Figs. 1 and 2). Although stress-induced redistribution of sHSPs is a well-known phenomenon as reported previously (*35, 43, 44*), the physiological significance of this phenomenon has not yet been elucidated. Fujimuro *et al.* reported that heat stress caused accumulation of ubiquitinated proteins in HeLa cells (*45*). Exposure to proteasome inhibitors also caused the accumulation of ubiquitinated proteins, especially in the insoluble fraction, in U373 MG cells under our experimental conditions (data not shown). From these observations, we suspect that sHSPs may interact with ubiquitinated proteins for proper folding or disruption of cellular proteins and accumulate preferentially in insoluble fraction under severe conditions such as heat stress or proteasome inhibition. It remains to be clarified whether sHSPs actually interact with ubiquitinated proteins.

HSP27 and αB-crystallin accumulated in aggresomes after treatment with proteasome inhibitors (Figs. 4 and 5), and to our knowledge, this is the first report of such colocalization of sHSPs. Proteasome inhibitor-induced reruitement of sHSPs to aggresomes is not restricted to the case of U373 MG cells, because recruitment of HSP27 to aggresomes was also observed in HeLa cells (Fig. 6A). Moreover, accumulation of αB-crystallin (Fig. 6B) and HSP27 (data not shown) in aggresomes induced by a misfolded protein, GFP-250 (*34*), was observed in NG108-15 cells. These results indicate that sHSPs are recruited to aggresomes induced by two different pathways, namely, proteasome inhibition and overexpression of misfolded proteins.

The physiological significance of recruitment of sHSPs to aggresomes is not clear, but other chaperones, HSP70 and HSP90, were found to be recruited into the centrosomal fraction after exposure to proteasome inhibitors and over-

expression of misfolded proteins in an earlier study (*46*). HSC70, HSP40 and the chaperonin TCP1 also co-localized in aggresomes induced by overexpression of misfolded proteins (*34*). Ehrnsperger *et al.* reported that HSP27 binds to non-native proteins, creates a reservoir of folding intermediates and allows refolding in cooperation with other chaperones (*47*). In the present study, ubiquitinated proteins and proteasomes also co-localized with sHSPs (Fig. 5, C and D, and data not shown). sHSPs and other chaperones may act in cooperation with each other to effect the conformation of misfolded and ubiquitinated proteins, and assist the degradation of misfolded and ubiquitinated proteins by proteasome in aggresomes. Chaperones like HSC70 (*48*) and Ydj1 (*49*) are reported to participate in the ubiquitin-dependent degradation of certain proteins, but it remains to be clarified whether this is also the case for sHSPs. On the other hand, sHSPs are known to interact with intermediate filaments and affect their filament formation and assembly (*50–52*). Moreover, it is reported that overexpression of glial fibrillary acidic protein (GFAP) in astrocytes induces formation of cytoplasmic inclusions, which are disaggregated by co-expression of αB-crystallin (*53*). We speculate that sHSPs may affect the structure of intermediate filaments during exposure to proteasome inhibitors and at least partially participate in the formation of cage-like structures of aggresomes.

Exposure to MG-132 caused activation of p38 and p44/42 MAP kinases in U373 MG cells (Fig 8) and phosphorylation of HSP27 and αB-crystallin (Figs. 7 and 9). HSP27 is reported to be phosphorylated by several downstream kinases of p38 MAP kinase, such as MAPKAP kinase-2/3 (*41, 54*) and PRAK (*42*). We previously reported that phosphorylation of Ser-59 in αB-crystallin is catalyzed by MAPKAP kinase-2, while phosphorylation of Ser-45 in αB-crystallin is catalyzed by p44/42 MAP kinase (*40*). In fact, SB203580 and PD169316, inhibitors of p38 MAP kinase, significantly but not completely inhibited MG-132-induced phosphorylation of HSP27 (Fig. 9A) and Ser-59 in αB-crystallin (Fig. 9B). Uo126 and PD98059, inhibitors of MEK, which activate p44/42 MAP kinase, did not inhibit MG-132–induced phosphorylation of HSP27 and Ser-59 in αB-crystallin but inhibited phosphorylation of Ser-45 in the latter (Fig. 9B and data not shown) These results suggest that proteasome inhibitors induce activation of p38 MAP kinase and p44/42 MAP kinase pathways in U373 MG cells and that this leads to phosphorylation of the small heat shock proteins, HSP27 and αB-crystallin.

SB203580 and PD98059 barely affected the accumulation of HSP27 and αB-crystallin or the formation of aggresomes by proteasome inhibitors (Figs. 9 and 10 and data not shown) These results indicate that phosphorylation is not required for the observed responses of HSP27 and αB-crystallin in U373 MG cells. Clarification of the mechanism involved in the formation of aggresomes and roles of HSP27 and αB-crystallin may lead to understanding of the pathology of several neurodegenerative diseases.

We thank Dr. Keiji Tanaka for the generous gift of monoclonal antibody to 20S proteasomes.

REFERENCES

1 Wickner, S., Maurizi, M.R., and Gottesman, S (1999) Post-translational quality control: folding, refolding, and degrading proteins. *Science* **286**, 1888–1893
2 Sherman, M.Y. and Goldberg, A.L. (2001) Cellular defenses against unfolded proteins: a cell biologist thinks about neurodegenerative diseases. *Neuron* **29**, 15–32
3 Hartl, F.U. (1996) Molecular chaperones in cellular protein folding *Nature* **381**, 571–579
4 Caspers, G.J., Leunissen, J.A., and de Jong, W.W. (1995) The expanding small heat-shock protein family, and structure predictions of the conserved "alpha-crystallin domain" *J. Mol. Evol.* **40**, 238–248
5 Klemenz, R., Fröhli, E., Steiger, R.H., Schäfer, R., and Aoyama, A. (1991) αB-crystallin is a small heat shock protein *Proc. Natl. Acad. Sci. USA* **88**, 3652–3656
6 Kato, K., Goto, S., Hasegawa, K., and Inaguma, Y. (1993) Coinduction of two low-molecular-weight stress proteins, αB crystallin and HSP28, by heat or arsenite stress in human glioma cells *J. Biochem.* **114**, 640–647
7 Arrigo, A.-P. (1990) Tumor necrosis factor induces the rapid phosphorylation of the mammalian heat shock protein hsp28 *Mol. Cell. Biol.* **10**, 1276–1280
8 Landry, J., Chretinen, P., Laszlo, A., and Lambert, H. (1991) Phosphorylation of HSP27 during development and decay of thermotolerance in Chinese hamster cells. *J. Cell. Physiol.* **147**, 93–101
9 Shinohara, H., Inaguma, Y., Goto, S., Inagaki, T., and Kato, K. (1993) αB crystallin and HSP28 are enhanced in the cerebral cortex of patients with Alzheimer's disease *J. Neurol. Sci.* **119**, 203–208
10 Goldman, J.E. and Corbin, E. (1991) Rosenthal fibers contain ubiquitinated αB-crystallin *Am. J. Pathol.* **139**, 933–938
11. Iwaki, T., Kume-Iwaki, A., Liem, R.K.H., and Goldman, J.E. (1989) αB crystallin is expressed in non-lenticular tissues and accumulates in Alexander's disease brain *Cell* **57**, 71–78
12 Mann, E., McDermott, M.J., Goldman, J., Chiesa, R., and Spector, A. (1991) Phosphorylation of alpha-crystallin B in Alexander's disease brain *FEBS Lett.* **294**, 133–136
13 Coux, O., Tanaka, K., and Goldberg, A.L. (1996) Structure and functions of the 20S and 26S proteasomes. *Annu. Rev. Biochem.* **65**, 801–847
14 Ciechanover, A. (1998) The ubiquitin-proteasome pathway: on protein death and cell life. *EMBO J.* **17**, 7151–7160
15 Rock, K.L., Gramm, C., Rothstein, L., Clark, K., Stein, R., Dick, L., Hwang, D., and Goldberg, A.L. (1994) Inhibitors of the proteasome block the degradation of most cell proteins and the generation of peptides presented on MHC class I molecules *Cell* **78**, 761–771
16 Fenteany, G., Standaert, R.F., Lane, W.S., Choi, S., Corey, E.J., and Schreiber, S.L. (1995) Inhibition of proteasome activities and subunit-specific amino-terminal threonine modification by lactacystin. *Science* **268**, 726–731
17 Kawazoe, Y., Nakai, A., Tanabe, M., and Nagata, K. (1998) Proteasome inhibition leads to the activation of all members of the heat-shock-factor family *Eur. J. Biochem.* **255**, 356–362
18 Mathew, A., Mathur, S.K., and Morimoto, R.I. (1998) Heat shock response and protein degradation regulation of HSF2 by the ubiquitin-proteasome pathway *Mol. Cell. Biol.* **18**, 5091–5098
19 Bush, K.T., Goldberg, A.L., and Nigam, S.K. (1997) Proteasome inhibition leads to a heat-shock response, induction of endoplasmic reticulum chaperones, and thermotolerance. *J. Biol. Chem.* **272**, 9086–9092
20. Meriin, A.B., Gabai, V.L., Yaglom, J., Shifrin, V.I., and Sherman, M.Y. (1998) Proteasome inhibitors activate stress kinases and induce Hsp72. Diverse effects on apoptosis. *J. Biol. Chem.* **273**, 6373–6379
21. Kim, D., Kim, S.H., and Li, G.C. (1999) Proteasome inhibitors MG132 and lactacystin hyperphosphorylate HSF1 and induce hsp70 and hsp27 expression *Biochem. Biophys. Res. Commun.* **254**, 264–268
22 Johnston, J.A., Ward, C.L., and Kopito, R.R. (1998) Aggresomes: a cellular response to misfolded proteins. *J. Cell. Biol.* **143**,

1883–1898
23. Kumatori, A., Tanaka, K., Inamura, N., Sone, S, Ogura, T, Matsumoto, T, Tachikawa, T, Shin, S, and Ichihara, A. (1990) Abnormally high expression of proteasomes in human leukemic cells. *Proc. Natl Acad Sci USA* **87**, 7071–7075
24 Yoshitake, S, Yamada, Y., Ishikawa, E, and Masseyeff, R (1979) Conjugation of glucose oxidase from *Aspergillus niger* and rabbit antibodies using *N*-hydroxysuccinimide ester of *N*-(4-carboxycyclohexylmethyl)-maleimide. *Eur J Biochem.* **101**, 395–399
25 Kato, K., Shinohara, H, Kurobe, N, Inaguma, Y, Shimizu, K., and Ohshima, K. (1991) Tissue distribution and developmental profiles of immunoreactive αB crystallin in the rat determined with a sensitive immunoassay system *Biochim Biophys. Acta* **1074**, 201–208
26 Laemmli, U.K. (1970) Cleavage of structural proteins during the assembly of the head of bacteriophage T4 *Nature* **227**, 680–685
27 O'Farrell, PH (1975) High resolution two-dimensional electrophoresis of proteins *J Biol Chem* **250**, 4007–4021
28 Ito, H, Okamoto, K., Nakayama, H, Isobe, T, and Kato, K. (1997) Phosphorylation of αB-crystallin in response to various types of stress. *J Biol Chem* **272**, 29934–29941
29 Kato, K., Shinohara, H, Goto, S, Inaguma, Y, Morishita, R., and Asano, T (1992) Copurification of small heat-shock protein with αB-crystallin from human skeletal muscle *J Biol Chem.* **267**, 7718–7725
30 Ito, H, Hasegawa, K., Inaguma, Y, Kozawa, O, and Kato, K. (1996) Enhancement of stress-induced synthesis of hsp27 and αB crystallin by modulators of the arachidonic acid cascade. *J Cell Physiol* **166**, 332–339
31 Cooper, L F and Uoshima, K. (1994) Differential estrogenic regulation of small Mr heat shock protein expression in osteoblasts *J Biol Chem* **269**, 7869–7873
32 Quax-Jeuken, Y, Quax, W, van Rens, G, Khan, PM, and Bloemendal, H (1985) Complete structure of the αB-crystallin gene Conservation of the exon-intron distribution in the two non-linked α-crystallin genes *Proc. Natl Acad Sci USA* **82**, 5819–5823
33 Ito, H, Kamei, K., Iwamoto, I, Inaguma, Y, Nohara, D, and Kato, K. (2001) Phosphorylation-induced change of the oligomerization state of αB-crystallin *J Biol Chem* **276**, 5346–5352
34 García-Mata, R., Bebok, Z, Sorscher, E J, and Sztul, E S (1999) Characterization and dynamics of aggresome formation by a cytosolic GFP-chimera *J Cell Biol* **146**, 1239–1254
35 Arrigo, A.P, Suhan, J P, and Welch, W J (1988) Dynamic changes in the structure and intracellular locale of the mammalian low-molecular-weight heat shock protein *Mol Cell. Biol* **8**, 5059–5071
36 Inaguma, Y., Goto, S., Shinohara, H, Hasegawa, K., Ohshima, K., and Kato, K. (1993) Physiological and pathological changes in levels of two small stress proteins, hsp27 and αB crystallin, in rat hindlimb muscles. *J Biochem* **114**, 378–384
37 Tsubuki, S, Saito, Y., Tomioka, M, Ito, H, and Kawashima, S (1996) Differential inhibition of calpain and proteasome activities by peptidyl aldehydes of di-leucine and tri-leucine. *J Biochem.* **119**, 572–576
38 Kristofferson, D., Mitchison, T, and Kirschner, M (1986) Direct observation of steady-state microtubule dynamics. *J Cell Biol* **102**, 1007–1019
39 Stokoe, D, Campbell, D.G., Nakielny, S., Hidaka, H, Leevers, S J, Marshall, C, and Cohen, P. (1992) MAPKAP kinase-2, a novel protein kinase activated by mitogen-activated protein kinase *EMBO J* **11**, 3985–3994
40 Kato, K., Ito, H, Kamei, K., Inaguma, Y, Iwamoto, I, and Saga, S (1998) Phosphorylation of αB crystallin in mitotic cells and identification of enzymatic activities responsible for phosphorylation *J Biol Chem* **273**, 28346–28354
41 McLaughlin, M M, Kumar, S, McDonnell, PC, Van Horn, S, Lee, J C, Livi, G P, and Young, P R (1996) Identification of mitogen-activated protein (MAP) kinase-activated protein kinase-3, a novel substrate of CSBP/p38 MAP kinase. *J Biol Chem.* **271**, 8488–8492
42 New, L, Jiang, Y, Zhao, M, Liu, K., Zhu, W, Flood, L J, Kato, Y, Parry, G C, and Han, J (1998) PRAK, a novel protein kinase regulated by the p38 MAP kinase. *EMBO J* **17**, 3372–3384
43 Inaguma, Y, Shinohara, H, Goto, S, and Kato, K. (1992) Translocation of αB crystallin by heat-shock in rat glioma (GA-1) cells *Biochem Biophys. Res. Commun* **182**, 844–850
44 Kato, K., Goto, S, Hasegawa, K., Shinohara, H, and Inaguma, Y (1993) Responses to heat shock of αB crystallin and HSP28 in U373 MG human human glioma cells. Biochim *Biophys. Acta* **1175**, 257–262
45 Fujimuro, M, Sawada, H, and Yokosawa, H (1997) Dynamics of ubiquitin conjugation during heat-shock response revealed by using a monoclonal antibody specific to multi-ubiquitin chains *Eur. J Biochem* **249**, 427–433
46 Wigley, W C, Fabunmi, R P, Lee, M G, Marino, C R, Muallem, S, DeMartino, G N, and Thomas, P J (1999) Dynamic association of proteasomal machinery with the centrosome *J Cell Biol* **145**, 481–490
47 Ehrnsperger, M, Graber, S, Gaestel, M, and Buchner, J (1997) Binding of non-native protein to Hsp25 during heat shock creates a reservoir of folding intermediates for reactivation *EMBO J* **16**, 221–229
48 Bercovich, B, Stancovski, I, Mayer, A., Blumenfeld, N, Laszlo, A., Schwartz, A.L, and Ciechanover, A (1997) Ubiquitin-dependent degradation of certain protein substrates in vitro requires the molecular chaperone Hsc70 *J Biol Chem* **272**, 9002–9010
49 Lee, D H, Sherman, M Y, and Goldberg, A.L (1996) Involvement of the molecular chaperone Ydj1 in the ubiquitin-dependent degradation of short-lived and abnormal proteins in Saccharomyces cerevisiae *Mol. Cell Biol* **16**, 4773–4781
50 Nicholl, I D and Quinlan, R.A. (1994) Chaperone activity of α-crystallins modulates intermediate filament assembly *EMBO J* **13**, 945–953
51. Djabali, K., de Nechaud, B, Landon, F, and Portier, M.M (1997) αB-crystallin interacts with intermediate filaments in response to stress. *J Cell Sci* **110**, 2759–2769
52 Perng, M D, Cairns, L, van den IJssel, P, Prescott, A., Hutcheson, A.M, and Quinlan, R.A. (1999) Intermediate filament interactions can be altered by HSP27 and alphaB-crystallin. *J Cell Sci* **112**, 2099–2112
53 Koyama, Y and Goldman, J E (1999) Formation of GFAP cytoplasmic inclusions in astrocytes and their disaggregation by αB-crystallin *Am J Pathol* **154**, 1563–1572
54 Stokoe, D, Engel, K., Campbell, D G, Cohen, P, and Gaestel, M (1992) Identification of MAPKAP kinase 2 as a major enzyme responsible for the phosphorylation of the small mammalian heat shock proteins *FEBS Lett* **313**, 307–313